Real time detection of DNA·RNA hybridization in living cells

(molecular beacon/antisense/oligodeoxynucleotide/fluorescence resonance energy transfer)

Deborah L. Sokol*†, Xiaolin Zhang‡, Ponzy Lu‡, and Alan M. Gewirtz*§¶

Departments of §Internal Medicine, *Pathology and Laboratory Medicine, and ‡Chemistry, University of Pennsylvania, 422 Curie Boulevard, Philadelphia, PA 19104

ABSTRACT Demonstrating hybridization between an antisense oligodeoxynucleotide and its mRNA target has proven to be extremely difficult in living cells. To address this fundamental problem in antisense research, we synthesized "molecular beacon" (MB) reporter oligodeoxynucleotides with matched fluorescent donor and acceptor chromophores on their 5′ and 3′ ends. In the absence of a complementary nucleic acid strand, the MB remains in a stem–loop conformation where fluorescence resonance energy transfer prevents signal emission. On hybridization with a complementary sequence, the stem–loop structure opens increasing the physical distance between the donor and acceptor moieties thereby reducing fluorescence resonance energy transfer and allowing a detectable signal to be emitted when the beacon is excited by light of the appropriate wavelength. Solution hybridization studies revealed that in the presence of a complementary strand targeted MB could yield up to a 60-fold increase in fluorescence intensity in comparison to control MB. By using a fluorescence microscope fitted with UV fluoride lenses, the detection limit of preformed MB/target sequence duplexes microinjected into cells was found to be $\geq 1 \times 10^{-1}$ ag of MB, or ~10 molecules of mRNA. On the basis of this exquisite sensitivity, real-time detection of MB/target mRNA hybridization in living cells was attempted by microinjecting MB targeted to the *vav* protooncogene, or control MB, into K562 human leukemia cells. Within 15 min, confocal microscopy revealed fluorescence in cells injected with targeted, but not control, MB. These studies suggest that real-time visualization and localization of oligonucleotide/mRNA interactions is now possible. MB could find utility in studying RNA processing, trafficking, and folding in living cells. We hypothesize that MB may also prove useful for finding targetable mRNA sequence under physiologic conditions.

Antisense oligodeoxynucleotides (AS ODNs) are being evaluated for treatment efficacy of viral (1), cardiovascular (2, 3), gastrointestinal (4, 5), and neoplastic diseases (6–8). The ODNs are thought to perturb gene expression by hybridizing with their complementary mRNA, thereby promoting translation arrest or, perhaps more likely, physical destruction of the mRNA by an RNase H-dependent mechanism (9–11). Nevertheless, studies that provide direct physical evidence for ODN/mRNA hybridization *in vivo* are rare. Decrement in targeted mRNA levels (12–14) or down-regulation of targeted protein (15–18) is widely used to infer duplex formation but RNA fragments consistent with ODN-guided cleavage have been described only in *Xenopus* oocytes (19) and hematopoietic cells (10). Whether such fragments truly represent the result of hybridization in the living cell is uncertain. Because it is widely appreciated that ODN may effect a multitude of

cellular process through mechanisms that do not involve hybridization with a specific mRNA (20, 21), this issue is clearly at the core of all "antisense" research.

To demonstrate ODN/mRNA hybridization *in vivo,* we were attracted to methods using fluorescence resonance energy transfer (FRET) (22, 23). The principle of FRET is based on transfer of electronic excitation energy through dipole–dipole coupling of a fluorescent donor to an acceptor. Transfer efficiency depends on donor and acceptor transition dipole orientation, distance between the molecules, and spectral properties of the donor and acceptor. FRET has been used to detect duplex formation between complementary ODN in solution (24–28) and within living cells (29). However, a potential problem with FRET-detected hybridization is that other phenomena may lead to loss of cellular fluorescence. Therefore, in a living cell one cannot be certain that loss of signal means conclusively that hybridization has actually taken place. The "molecular beacon" (MB) concept of Tyagi and Kramer (30, 31) addresses this concern. These molecules have a stem–loop structure with fluorophore and quenching moieties annealed to the 5′ and 3′ ends of the molecule, respectively (Fig. 1). The fluorophore does not modify the structure of the hairpin (32) thereby permitting the loop sequence to hybridize with its respective complementary nucleic acid sequence. Once duplex formation occurs, the fluorophore and quencher become separated in space and FRET is no longer possible. The fluorophore will then emit light of the appropriate wavelength when excited. This event is readily detected in solution by use of a fluorimeter or by direct observation using a suitably equipped microscope. We demonstrate herein that MBs can be used to directly demonstrate duplex formation in living cells.

MATERIALS AND METHODS

Cell Lines. TK⁻ts13 (hamster fibroblasts), and K562 human leukemia cells were obtained from the American Type Culture Collection.

Synthesis of MBs. MBs were synthesized as described (30) and are illustrated in Fig. 1. The 5′ fluorophore donor used was EDANS [5-(2′-aminoethyl)aminonapthalene-1-sulfonic acid]. DABCYL [4-(4′-dimethylaminophenylazo) benzoic acid] was used as the 3′ acceptor. "Stem" structures were formed by the same complementary 5′ (GCGAG) and 3′ (CTCGC) nucleotides. These flanked the following loop sequences: vav AS, GTTCTTAAGGCACAGGAACTGGGA; β-actin AS, CGCGGCGATATCATCATCCATAAC; vav sense control, TCCCAGTTCCTGTGCCTTAAGAAC; β-actin sense con-
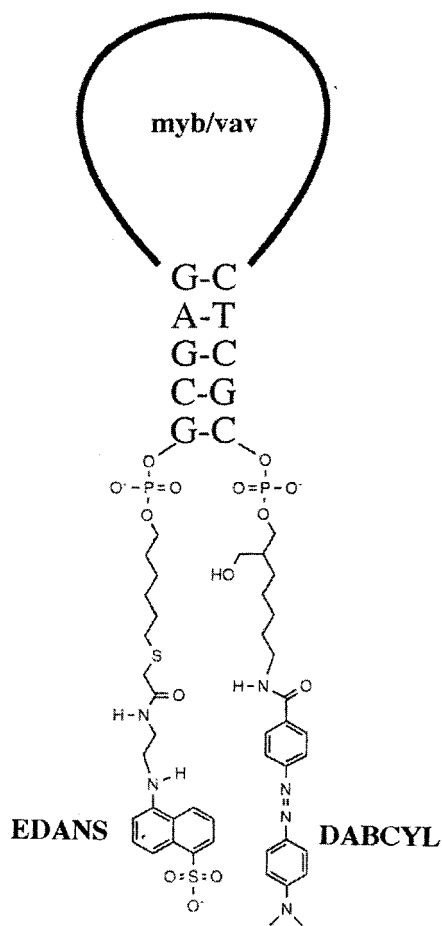
FIG. 1. MB structure. MBs were synthesized with a 24-nt "loop" sequence flanked on the 5′ and 3′ ends with complementary sequence 5 nt long. Internal hybridization of the complementary ends creates the stem–loop structure. The fluorescent donor (EDANS) and acceptor (DABCYL) molecules are joined to the 5′ terminal phosphate and the 3′ terminal hydroxyl group, respectively, through (CH2)6-S-CH2-CO and (CH2)7-NH linker arms.

trol, GTTATGGATGATGATATCGCCGCG; vav Scrambled (SCR) control, AGACCTGGTTGTTCACGGGAAAAG; β-actin SCR control, GGTAGATGCAGCCTTGTCTAT-ACC; vav mismatch control, GTTCTTAACCGTGTC-GAACTGGGA; β-actin mismatch control, CGCGGCGAT-AGGTACATCCATAAC.

Fluorescence Detection of Hybrid Formation. AS or control MB (final concentration, 150–200 nM) dissolved in MB buffer (100 mM Tris·HCl, pH 8/1 mM MgCl$_2$) was added to an excess of complementary target ODN (20–30 μM). Fluorescence emission was monitored in a Hitachi/Perkin–Elmer MPF4 spectrofluorimeter. Controls were composed of a 6-bp mismatch, SCR, or sense (SEN) loop sequences. The excitation wavelength of EDANS was 336 nm, and the emission maximum was 490 nm. The efficiency of FRET between the donor and acceptor was recorded by scanning the emission spectra from 375 nm to 525 nm for the EDANS/DABCYL pair after excitation at 336 nm in a fluorimeter. In all experiments, the background fluorescence intensity of the MB buffer was negligible as was the background fluorescence of described controls when sense target sequences were added to the solution. Each MB was evaluated for fluorescence emission after addition of its complementary target sequence.

Electrophoretic Analysis. Samples containing AS-MB/sense ODN duplexes, as well as control MB with this same template, were analyzed on nondenaturing 8% polyacrylamide gels. After electrophoresis of samples at 70 V for 1.5 h, gels

were soaked in a solution of ethidium bromide at 50 μg/ml and examined on a UV light box. The mobility of duplexed material was retarded on these gels in comparison to unduplexed material.

DNase I Action. A sample containing unhybridized MB was equilibrated at 37°C and then 5 μl of DNase I (Boehringer Mannheim) enzyme was added in DNase I buffer (400 mM Tris·HCl, pH 7.4/100 mM NaCl/60 mM MgCl$_2$/100 mM CaCl$_2$). The fluorescence emission of these solutions was monitored through fluorimetric scans as described above.

Hybridization to Total RNA. Total RNA was extracted from hematopoietic K562 cells as described (33). RNA (3 μg) was heated to 95°C for 5 min and then hybridized to AS or control MBs. After hybridization overnight at 37°C, 0.6 ml of Tris buffer containing 1 mM Mg Cl$_2$ was added, and samples were centrifuged for 20 min to remove particulate matter. The scanning emission spectra in a fluorimeter was completed as described.

Microinjection of MBs and Preformed Duplexes. K562 cells were centrifuged at 300 rpm for 10 min onto cytospin slides that had been treated with CELL-TAK (Collaborative Bio-Medical Products, Bedford, MA). Rings were immediately drawn with a hydrophobic PAP pen (Kiyota International, Elk Grove Village, IL) and RPMI 1640 medium supplemented with 10% bovine calf serum was dropped into the ring to ensure survival of the cells. Slides were viewed under an IMT-2 inverted microscope while performing microinjection. Approximately 10–100 pl of MBs, resuspended in MB buffer, was injected per cell. Approximately 100–200 microinjections were completed within 10 min. Slides were coverslipped and immediately exposed to UV light for 50 s. Images were grabbed with a KS-1381 Videoscope (Videoscope International, Washington, DC) and fluorescence levels were measured by using CUE series image analysis software, with reference to uniformly dyed microspheres of 19.5 μM diameter (product LF97371/171–1, Bangs Laboratories, Carmel, IN).

Alternatively to grabbing images, 35-mm slide film was exposed to the images with an Olympus C-35AD-4 35-mm camera with an attached exposure control unit set on automatic. Photographic images were also captured at various time intervals, at different exposure settings that were then recorded.

Confocal Laser Scanning Microscopy. A Leitz confocal laser scanning module attached to an inverted microscope was used to monitor fluorescence emission. This microscope was equipped with a broad-range UV lens that stimulates at a wavelength of 351 nm. To optimize the UV fluorescence emission, the 440–40 long-pass filter was set to channel 1. The long-pass 450 filter was set to channel 2, and the substrate was set to dichroic so that all fluorescent energy was sent to channel 2. To prevent photobleaching, the confocal microscope was operated under conservative conditions (low illumination and intermediate slit positions., 14–25 μm, to maximize signal strength).

RESULTS

MB Design. A 34-nt MB stem–loop structure composed of 5-nt complementary flanking sequences and a 24-nt intervening loop sequence was synthesized (Fig. 1). EDANS, the fluorescent donor, and DABCYL, the acceptor, were conjugated to the 5′ and 3′ ends of the molecule, respectively, through spacer arms. The major nucleic acid sequence constraints for MB design have been reported (30). They presume that the molecule assumes a stem–loop structure in the absence of a complementary sequence. In the stem–loop configuration, the EDANS and DABCYL moieties are in close enough proximity so that FRET occurs and no fluorescent signal is observed. In the presence of a complementary target sequence, a bimolecular helix is formed causing the stem–loop

structure to open. The fluorophore and quenching moieties then move far enough apart in space so that FRET is diminished or nonexistent. A detectable signal may then be emitted upon excitation of the fluorescence donor group on the MB molecule.

To test these predictions, MBs with different loop sequences were mixed in solution with a variety of ODN target sequences, excited by UV light (336-nm peak wavelength), and then examined by a spectrofluorimeter for the emission signal. Sequences used were given above. As expected, fluorescence signal was detected only when MBs were placed in solution with the ODN target to which they could hybridize (Fig. 2). For example, when an ~137-fold molar excess of a target ODN corresponding to vav nucleotides 195–218, or β-actin nucleotides 8–31, was incubated at room temperature with MBs containing loops corresponding to either vav or β-actin AS, SCR, or mismatched (vav-7 and β-actin-4 nucleotides) sequence, fluorescence signal was observed only when the target ODNs and MBs were complementary to each other (Fig. 2
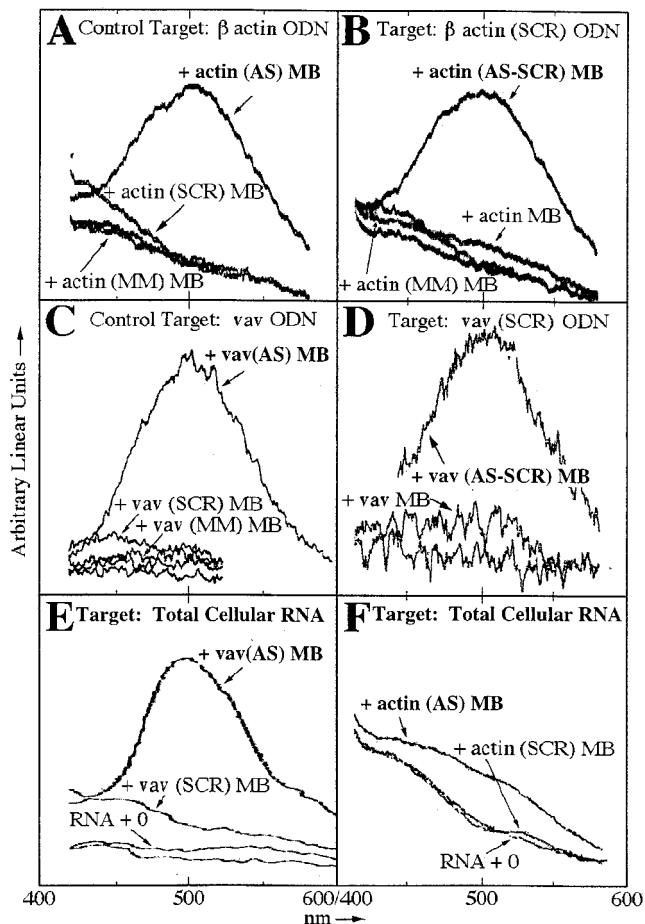

A–D). The specificity of these reactions is worth emphasizing. Signal above background was never detected when target sequence and MB were mismatched at four or more bases.

Interestingly, fluorescence signal intensity varied with the target/MB pair used (Fig. 2 A–D). For vav target/MB duplexes, for example, a signal ~30 times greater than background was observed, a result consistent with beacon fluorescence intensity reported by Tyagi and Kramer (30, 31). In contrast, β-actin/MB duplexes generated signal only ~15 times greater than background. These differences might be explained by the nature of the intramolecular folding and/or hybridization permitted by the MB sequence used. Such folding could impact on hybridization efficiency with consequent effects on output signal. It is important to note that when MB sequences were digested with DNase I, full fluorescence emission was observed in the fluorimeter (data not shown). Accordingly, the results in aggregate strongly suggest that the predicted stem–loop structures were in fact forming and that, when DNA sequence complementary to the MB loop structure was added to the reaction, the anticipated hybridization induced conformational change took place, leading to fluorescence detection in an appropriately excited sample.

We also examined the ability of the various MBs to hybridize with target in a pool of total cellular RNA. RNA was extracted from K562 cells and then mixed with AS sequence MBs or control nucleic acid sequence MBs. In comparison to control MB, we observed a 15-fold increase in fluorescence signal when AS-vav-MBs were allowed to hybridize with total K562 RNA (Fig. 2E). AS-β-actin MB showed a 9-fold rise in fluorescence emission in comparison to its controls (Fig. 2F), a result in accord with the data presented above.

Detection of Endogenous MB/mRNA Hybridization. By using serial dilutions of preformed MB/ODN duplexes microinjected into K562 cells, we found that we could detect as little as 1×10^{-1} ag of material, which corresponds to ~10 molecules of AS vav MB. If the average cell is 10^{-12}–10^{-11} liters, we calculate that we can detect 20–200 pM RNA. On the basis of these calculations, we hypothesized that we would be able to detect MB/mRNA hybridization, real time, in living cells. We tested this prediction by microinjecting 150 μM *vav* AS or SCR (control) MBs into living K562 human leukemia cells. After injection, the cells were examined for signal by phase and fluorescence microscopy (Fig. 3). Higher levels of cellular fluorescence were observed in cells injected with AS MB (Fig. 3 C and D) than in those cells injected with SCR MBs (Fig. 3 A and B). Uninjected cells displayed no discernible fluorescence (Fig. 3 E and F). Specificity of the fluorescence signal was further determined by injecting fibroblasts with AS MBs or vav(SCR) MBs. Both were comparable in fluorescence with vav SCR MB-injected K562 controls. In marked contrast however, cells injected with β-actin AS MBs had a fluorescence signal that was twice the intensity of the control cells (data not shown).

We quantified the intensity of fluorescent signals emitted from MB/mRNA duplexes by using CUE series image analysis software. Fluorescence intensity of AS-*vav*-MB complexed to target mRNA was approximately 2.2-fold higher than sequence matched controls relative to a manufactured fluorescent standard (Bangs Laboratories; Fig. 4). The fluorescence intensity of AS-MB targeting β-actin sequences was approximately 5.5 fold higher than matched controls. This result was anticipated because β-actin mRNA is expressed at higher copy number than vav. Approximately 50 cells were injected with either AS or control MB and examined for fluorescence emission within each experiment. The experiment was repeated three times and data are reported as the mean ± SD.

We then attempted to more finely localize the intracellular location(s) of MB/mRNA duplex formation by using confocal microscopy. AS and control MBs were injected into living cells which were then examined as described in the methods (Fig. 5).

FIG. 2. Specificity of AS MB double helical and hybrid formation in solution. (*A–D*) Fluorescence emission spectra when various MB sequences were added to solutions of target ODNs. Hybridization was detected by spectrofluorimetry. Excitation wavelength was 336 nm. Signal intensity is displayed along the vertical axis, and the wavelength scanned is displayed on the horizontal axis. An increase in fluorescence intensity, ranging from 15- to 60-fold in comparison to background, was only observed with complementary MB/oligonucleotide pairs. Lowest baselines are tracings derived from solutions containing buffer or ODNs only. (*E* and *F*) Spectrofluorimetric tracings derived from AS-MB or SCR-MB, no MB, or MB buffer only incubated with total RNA extracted from K562 hematopoietic cell lines. Addition of MBs complementary to vav (*E*) or β-actin (*F*) mRNA sequence resulted in 15- and 9-fold increases in fluorescence intensity respectively in comparison to controls.
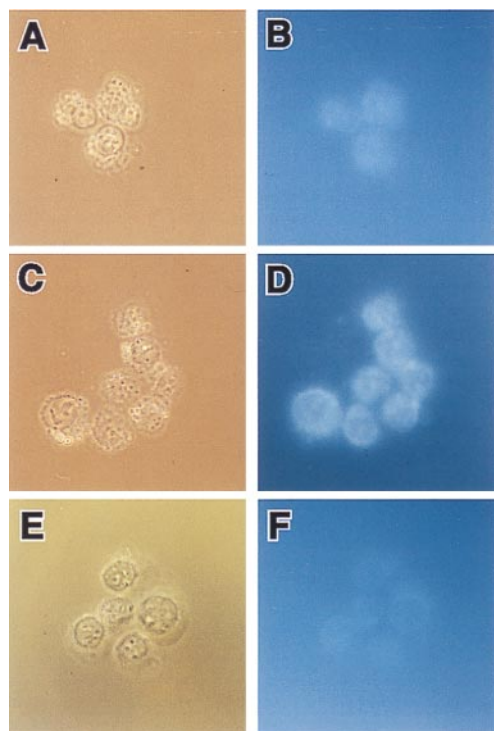
FIG. 3. Fluorescence emission of MB after microinjection into K562 hematopoietic cells. After injection of 150 μM vav AS or SCR (control) MBs into living K562 human leukemia cells, the cells were examined for signal by phase (*A*, *C*, and *E*) and corresponding fluorescence (*B*, *D*, and *F*) microscopy. Significantly higher levels of cellular fluorescence were observed in cells injected with AS MBs (*C* and *D*) than in those cells injected with SCR MBs (*A* and *B*). Uninjected cells displayed no fluorescence (*E* and *F*). *A* shows uninjected control cells photographed under phase microscopy; *B* is the corresponding fluorescent photomicrograph. *C* and *E* are AS-MB- and SCR-MB-injected K562 cells, respectively, photographed under phase microscopy, and *D* and *F* are their corresponding fluorescent counterparts, respectively. Note that maximal fluorescent emission is found in AS-MB-injected cells.

Little or no signal was observed in cells injected with control (SCR sequence) MB (data not shown). In contrast, cells injected with AS vav MBs revealed fluorescence signal when irradiated by a laser tuned to excite at 351 nm (Fig. 5). Considerably more fluorescence was observed in the area corresponding to the cell's cytoplasm than nucleus, suggesting that hybridization was favored in the latter location.

Speed and Integrity of AS-MB/mRNA Duplex Formation *in Vivo*. To gain an appreciation of the time course of hybridization between vav targeted AS MBs and their mRNA targets, we microinjected MBs into ~100 K562 cells under direct microscopic visualization by using a Narshige micromanipulator (Medical Systems, Greenvale, NY). All injections were accomplished within ~14 min after which the slides were coverslipped and illuminated with UV light for 50 s. The slides were then viewed with a fluorescence microscope equipped with UV fluoride lenses. Fluorescence was easily detectable in the AS-MB-injected cells although none was observed in cells injected with control MBs. Accordingly, these experiments indicate that the injected MBs find and hybridize with their endogenous mRNA target within 15 min of being introduced into the cell.

In additional experiments we noted that control MBs exposed to constant UV light also emitted fluorescent signals after approximately 45 min of excitation. We noted, however, that control MB exposed to constant UV light also emitted fluorescent signals after approximately 45 min of excitation. This observation suggests that intracellular nucleases may have degraded the MB hairpin-loop structure or that transient opening or "breathing" of the MB molecule was occurring. Either explanation is possible because fluorescence would not be observed in MBs that maintained their predicted conformation. Nonetheless, the apparent degradation of MB/target duplexes over time can be used to estimate the half-life of the MBs in an intracellular environment. From examination of more than 800 cells within eight experiments, phosphodiester MBs appear to undergo significant hydrolysis after ~45 min.

DISCUSSION

The goal of the studies described herein was to determine whether the MB strategy could be used to identify and quantify intracellular duplex formation between physiologically relevant mRNA species and appropriately targeted MB. For this purpose we synthesized MB with 5' fluorescent EDANS groups and a DABCYL quencher coupled to the 3' end. Loop sequences were designed to hybridize with endogenous vav mRNA, which encodes an important hematopoietic cell signaling protein (34), and the highly expressed housekeeping gene β-actin. The results of our studies demonstrate clearly that MB may be used to detect hybridization events *in vitro*. In solution, for example, we observed up to a 60-fold increase in fluorescence emission intensity when MBs hybridized to complementary ODNs in solution. In a more relevant model, up to a 15-fold increases in fluorescence intensity, in comparison to controls, was observed when MBs were allowed to hybridize with complementary sequences found in the total RNA fraction of K562 human leukemia cells. These results suggested that even in a large pool of competing mRNA species, specific detectable hybridization could take place.

The *in vitro* results described above further suggested the possibility of using MBs to monitor mRNA hybridization, real time, in living cells. We examined this possibility in an orderly fashion. First, preformed hybrids were microinjected into K562 cells to determine the possibility of detecting scarce to intermediate frequency target mRNA molecules (15–300 copies) within the cell. We found we could detect fluorescence signal from such complexes after injection of as little as 1×10^{-1} ag of material, or ~10 molecules of MB. Next, we microinjected 150 μM vav targeted AS or control MB into the nucleus of K562 cells. Cells injected with the AS molecule emitted detectable fluorescence ~2- to 5.5-fold higher than controls within 15 min. Specificity of these reactions was demonstrated in a number of ways including the use of numerous control MB injections, and injection of AS MBs into cells which do not express the targeted message. In all cases, signal clearly above background was observed only under those conditions in which it was expected, i.e., when the MB and its targeted complement were present in the cell under study.

The speed, and apparent integrity, of duplex formation was assessed by examining cells for fluorescence at specific time periods after microinjection. Hybridization appeared to occur within 15 min of introducing MB into the nucleus of K562 cells. Little or no detectable fluorescence was observed in cells injected with control MB at similar observation points. Detailed kinetics of hybridization within this time period are presently being examined. However, after ~45 min, fluorescence was observed in cells injected with control MBs. While MBs may be slightly more resistant to nucleases than linear ODNs because of the presence of the Mg-stabilized 5',3'-derivatized stem structure (30), we speculate that the appearance of fluorescence in control injected cells is likely the result of MB degradation. Alternatively, binding of proteins that destabilize the hairpin structure and cause it to open may also play a role in this effect (35–37).

MBs may be more fully stabilized by chemical modifications to the internucleotide linkages, which would provide greater nuclease resistance (38–40). In addition to modifications to
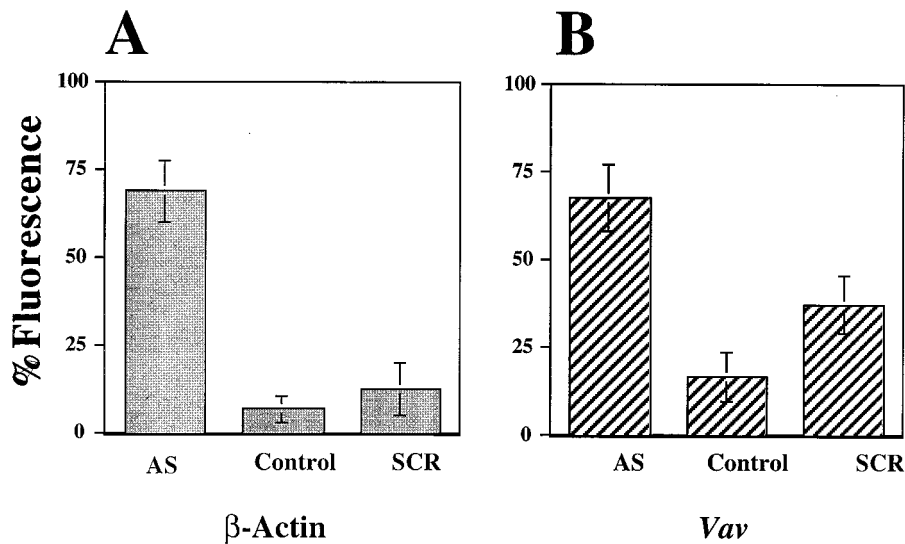
FIG. 4.   Relative fluorescence intensity of molecular beacons. K562 cells were microinjected with AS-, SCR-, or NO-β-actin (*A*) or *vav* (*B*) MBs at 150 μM. MBs hybridized to target sequences within 14 min. Cells were then exposed to UV light by using a $\times 60$ plan Apo numerical aperture 1.4 UV fluoride lens. Fluorescent signals were observed within 50 s, and images were captured with a KS-1381 videoscope. Fluorescence levels were measured by using CUE series image analysis software with reference to uniformly dyed microspheres.

the internucleoside bridge, sugar or base alterations may also be expected to lend increased stability to MBs (41–43). More stabilized molecules could reasonably be expected to generate higher signal to noise ratios. Higher levels of fluorescence might also be obtainable by redesigning loop sequence with impaired ability to undergo intramolecular folding. Alternatively, because mRNA associated proteins and/or tertiary structure may govern the ability of MBs to hybridize with their target, targeting different portions of the mRNA molecule might also be considered (8, 44). MB stabilization and higher signal to noise ratio would clearly be useful for more mechanistic studies on ODN sorting within cells and defining locations where duplex formation occurs most readily. We further speculate that MBs might prove useful for finding accessible

regions within an RNA molecule that one wished to target for destruction with an antisense oligonucleotide strategy.

In addition to direct visualization of ODN/mRNA duplex formation, stabilized MBs with strongly emitting fluorophore moieties may lend insight into the mechanism of action of AS-ODNs within cells. For example, when target mRNA is processed in the nucleus and exported to the cytoplasm, an MB duplexed with the mRNA should allow this transition to be monitored real time by confocal fluorescence microscopy. If RNase H-assisted catalysis occurs in the nucleus, MB fluorescence would be lost in this location because of reformation of stem–loop sequences. The nuclei of effected cells would, therefore, appear dark. Alternatively, if RNase H-mediated degradation of the mRNA duplex does not occur, and the MB/mRNA hybrid is transported to the cytoplasm, it should be possible to demonstrate complex colocalization with ribosomes and possibly interference with translation if fluorescent signals remain in the same intracellular location. Other uses for the MBs might easily be contemplated including their use to study mRNA folding and processing, *in vivo*. MB might also act as reporters of viral invasion or the presence of mutated mRNA transcripts *in vivo*. With optimization of MB stability and fluorescence emission, these molecules should become valuable tools for studying many aspects of RNA biology in living cells.
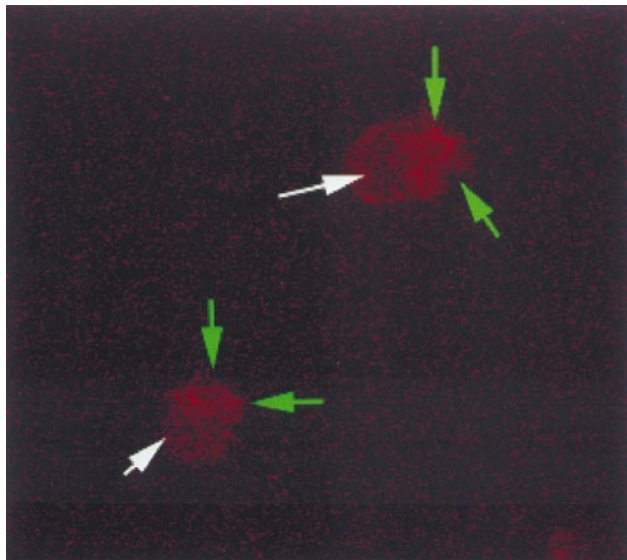
FIG. 5.   Confocal image of K562 cells injected with AS vav MBs. Cells injected with AS vav MBs revealed fluorescence signal when irradiated by a laser tuned to excite at 351 nm. Fluorescence images were gathered 15–30 min after MB injection and appeared stronger in the cells' cytoplasm (outlined by green arrows) than in the nucleus (white arrow), suggesting that hybridization may be favored in the latter location. Uninjected cells or cells injected with control MBs displayed little or no signal and were, therefore, very dark or unseen.

1. Leeds, J. M., Henry, S. P., Truong, L., Zutshi, A., Levin, A. A. & Kornbrust, D. (1997) *Drug Metab. Dispos.* **25,** 921–926.
2. Dzau, V. J., Morishita, R. & Gibbons, G. H. (1993) *Trends Biotechnol.* **11,** 205–210.
3. Morishita, R., Gibbons, G. H., Kaneda, Y., Ogihara, T. & Dzau, V. J. (1994) *Gene* **149,** 13–19.
4. Bold, R. J., Warren, R. E., Ishizuka, J., Cho-Chung, Y. S., Townsend, C. M., Jr. & Thompson, J. C. (1994) *Surgery* **116,** 189–195; discussion 195–196.
5. Chang, A. G. & Wu, G. Y. (1994) *Gastroenterology* **106,** 1076–1084.
6. Ho, P. T. & Parkinson, D. R. (1997) *Semin. Oncol.* **24,** 187–202.
7. Narayanan, R. & Akhtar, S. (1996) *Curr. Opin. Oncol.* **8,** 509–515.

8. Gewirtz, A. M., Stein, C. A. & Glazer, P. M. (1996) *Proc. Natl. Acad. Sci. USA* **93**, 3161–3163.
9. Giles, R. V., Ruddell, C. J., Spiller, D. G., Green, J. A. & Tidd, D. M. (1995) *Nucleic Acids Res.* **23**, 954–961.
10. Giles, R. V., Spiller, D. G. & Tidd, D. M. (1995) *Antisense Res. Dev.* **5**, 23–31.
11. Larrouy, B., Blonski, C., Boiziau, C., Stuer, M., Moreau, S., Shire, D. & Toulme, J. J. (1992) *Gene* **121**, 189–194.
12. Silvia, C. P., Jaber, M., King, G. R., Ellinwood, E. H. & Caron, M. G. (1997) *Neuroscience* **76**, 737–747.
13. Yamaguchi, K., Papp, B., Zhang, D., Ali, A. N., Agrawal, S. & Byrn, R. A. (1997) *AIDS Res. Hum. Retroviruses* **13**, 545–554.
14. Hijiya, N., Zhang, J., Ratajczak, M. Z., Kant, J. A., DeRiel, K., Herlyn, M., Zon, G. & Gewirtz, A. M. (1994) *Proc. Natl. Acad. Sci. USA* **91**, 4499–4503.
15. Boden, S. D., Hair, G., Titus, L., Racine, M., McCuaig, K., Wozney, J. M. & Nanes, M. S. (1997) *Endocrinology* **138**, 2820–2828.
16. Didier, M., Xu, M., Berman, S. A., Saido, T. C. & Bursztajn, S. (1997) *Neuroscience* **78**, 1129–1146.
17. Liu, Z. Z., Kumar, A., Ota, K., Wallner, E. I. & Kanwar, Y. S. (1997) *Proc. Natl. Acad. Sci. USA* **94**, 6758–6763.
18. Tari, A. M., Arlinghaus, R. & Lopez-Berestein, G. (1997) *Biochem. Biophys. Res. Commun.* **235**, 383–388.
19. Shuttleworth, J. & Colman, A. (1988) *EMBO J.* **7**, 427–434.
20. Chavany, C., Connell, Y. & Neckers, L. (1995) *Mol. Pharmacol.* **48**, 738–746.
21. Basu, S. & Wickstrom, E. (1997) *Nucleic Acids Res.* **25**, 1327–1332.
22. Wu, P. & Brand, L. (1994) *Anal. Biochem.* **218**, 1–13.
23. Yang, M. & Millar, D. P. (1997) *Methods Enzymol.* **278**, 417–444.
24. Perkins, T. A., Wolf, D. E. & Goodchild, J. (1996) *Biochemistry* **35**, 16370–1637.
25. Yang, M., Ghosh, S. S. & Millar, D. P. (1994) *Biochemistry* **33**, 15329–15337.
26. Mergny, J. L., Boutorine, A. S., Garestier, T., Belloc, F., Rougee, M., Bulychev, N. V., Koshkin, A. A., Bourson, J., Lebedev, A. V., Valeur, B., *et al.* (1994) *Nucleic Acids Res.* **22**, 920–928.
27. Ghosh, S. S., Eis, P. S., Blumeyer, K., Fearon, K. & Millar, D. P. (1994) *Nucleic Acids Res.* **22**, 3155–3159.
28. Jares-Erijman, E. A. & Jovin, T. M. (1996) *J. Mol. Biol.* **257**, 597–617.
29. Sixou, S., Szoka, F. C., Jr., Green, G. A., Giusti, B., Zon, G. & Chin, D. J. (1994) *Nucleic Acids Res* **22**, 662–668.
30. Tyagi, S. & Kramer, R. (1996) *Nat. Biotechnol.* **14**, 303–308.
31. Tyagi, S., Bratu, S. P. & Kramer, F. R. (1998) *Nat. Biotechnol.* **16**, 49–53.
32. Refregiers, M., Laigle, A., Jolles, B., Wheeler, G. & Chinsky, L. (1997) *Eur. Biophys. J.* **26**, 277–281.
33. Chomczynski, P. & Sacchi, N. (1987) *Anal. Biochem.* **162**, 156–159.
34. Clevenger, C. V., Ngo, W., Sokol, D. L., Luger, S. M. & Gewirtz, A. M. (1995) *J. Biol. Chem.* **270**, 13246–13253.
35. Nomura, Y., Ueno, Y. & Matsuda, A. (1997) *Nucleic Acids Res.* **25**, 2784–2791.
36. Monia, B. P., Johnston, J. F., Sasmor, H. & Cummins, L. L. (1996) *J. Biol. Chem.* **271**, 14533–14540.
37. Gamper, H. B., Reed, M. W., Cox, T., Virosco, J. S., Adams, A. D., Gall, A. A., Scholler, J. K. & Meyer, R. B., Jr. (1993) *Nucleic Acids Res.* **21**, 145–150.
38. Wagner, R. W. & Flanagan, W. M. (1997) *Mol. Med. Today* **3**, 31–38.
39. Zon, G. (1995) *Toxicol. Lett.* **82–83**, 419–424.
40. Crooke, S. T. (1997) *Adv. Pharmacol.* **40**, 1–49.
41. Lavignon, M., Tounekti, N., Rayner, B., Imbach, J. L., Keith, G., Paoletti, J. & Malvy, C. (1992) *Antisense Res. Dev.* **2**, 315–324.
42. Morvan, F., Porumb, H., Degols, G., Lefebvre, I., Pompon, A., Sproat, B. S., Rayner, B., Malvy, C., Lebleu, B. & Imbach, J. L. (1993) *J. Med. Chem.* **36**, 280–287.
43. Monia, B. P., Lesnik, E. A., Gonzalez, C., Lima, W. F., McGee, D., Guinosso, C. J., Kawasaki, A. M., Cook, P. D. & Freier, S. M. (1993) *J. Biol. Chem.* **268**, 14514–14522.
44. Dewanjee, M. K., Ghafouripour, A. K., Kapadvanjwala, M. & Samy, A. T. (1994) *Biotechniques* **16**, 844–846, 848, and 850.